AD_____

Award Number: W81XWH-04-1-0380

TITLE: INT6 May Influence Breast Cancer Formation by Regulating the 26S Proteasome

PRINCIPAL INVESTIGATOR: Zhe Sha, Ph.D.
Eric Chang, Ph.D.

CONTRACTING ORGANIZATION: Baylor College of Medicine
Houston, TX 77030

REPORT DATE: April 2007

TYPE OF REPORT: Annual Summary

PREPARED FOR: U.S. Army Medical Research and Materiel Command
Fort Detrick, Maryland 21702-5012

REPORT DOCUMENTATION PAGE

Form Approved
OMB No. 0704-0188

1. REPORT DATE *(DD-MM-YYYY)*	**2. REPORT TYPE**	**3. DATES COVERED** *(From - To)*
01-04-2007	Annual Summary	15 Mar 2004 – 14 Mar 2007

4. TITLE AND SUBTITLE

INT6 May Influence Breast Cancer Formation by Regulating the 26S Proteasome

5a. CONTRACT NUMBER

5b. GRANT NUMBER
W81XWH-04-1-0380

5c. PROGRAM ELEMENT NUMBER

6. AUTHOR(S)

Zhe Sha, Ph.D. and Eric Chang, Ph.D.

E-Mail: zsha@bcm.tmc.edu

5d. PROJECT NUMBER

5e. TASK NUMBER

5f. WORK UNIT NUMBER

7. PERFORMING ORGANIZATION NAME(S) AND ADDRESS(ES)

Baylor College of Medicine
Houston, TX 77030

8. PERFORMING ORGANIZATION REPORT NUMBER

9. SPONSORING / MONITORING AGENCY NAME(S) AND ADDRESS(ES)
U.S. Army Medical Research and Materiel Command
Fort Detrick, Maryland 21702-5012

10. SPONSOR/MONITOR'S ACRONYM(S)

11. SPONSOR/MONITOR'S REPORT NUMBER(S)

12. DISTRIBUTION / AVAILABILITY STATEMENT
Approved for Public Release; Distribution Unlimited

13. SUPPLEMENTARY NOTES – Original contains colored plates: ALL DTIC reproductions will be in black and white.

14. ABSTRACT
Inactivation of *int6* has been linked to breast cancer formation, but its molecular function and precise role in tumorigenesis are largely unknown. This project tests the hypothesis that *int6* is a tumor suppressor gene, regulating the proteasome to mediate genetic stability and cell division. My data showed that Int6 formed a complex with the proteasome. If *int6* expression is knocked down, proteasome becomes mis-assembled. These *int6*- cells are hypersensitive to proteasome drug and show chromosome instability. To better understand the mechanism through which *int6* regulates the proteasome, I have also completed a structure-function analysis to better understand the role of PCI domain in the Int6 protein and a manuscript describing this study has been submitted and under review. In addition to these progresses, I have just completed a photobleaching-based study analyzing proteasome mobility and movement *in vivo*, and how is this regulated by *int6*. A manuscript describing this will be submitted in a month. In conclusion, this fellowship has allowed me to work very productively to decipher the function of *int6* as a potential breast tumor suppressor.

15. SUBJECT TERMS
Int6, tumor suppressor gene, breast cancer, MCF10A, proteasome, genetic stability

16. SECURITY CLASSIFICATION OF:			**17. LIMITATION OF ABSTRACT**	**18. NUMBER OF PAGES**	**19a. NAME OF RESPONSIBLE PERSON**
a. REPORT	**b. ABSTRACT**	**c. THIS PAGE**			USAMRMC
U	U	U	UU	36	**19b. TELEPHONE NUMBER** *(include area code)*

Standard Form 298 (Rev. 8-98)
Prescribed by ANSI Std. Z39.18

Table of Contents

Page

Introduction

The *int6* gene was first discovered in a screen, in which the Mouse Mammary Tumor Virus (MMTV) was used as an insertional mutagen to discover genes important for breast cancer formation [1]. It was latter shown to be also important for breast tumorigenesis in humans [2-4]. However, its molecular function is poorly understood. Using the fission yeast *Schizosaccharomyces pombe* as a model system, we discovered an evolutionarily conserved function of Int6, which is to regulate the nuclear import, assembly, and proper functioning of the 26S proteasome [5-7]. These findings suggest that disruption of Int6 might lead to breast tumorigenesis in humans by weakening the 26S proteasome, leading to accumulation of regulatory proteins, some of which are essential for proper chromosome segregation and cell cycle progression. Thus, **this project investigates the hypothesis that a key function of Int6 is to control proteasome function, and this function is conserved in human to influence breast tumor formation.** The specific aims of this proposal are to determine whether disrupting Int6 function can influence (1) proteasome functioning and (2) chromosome segregation in human mammary epithelial cells. Mechanistic studies to understand the molecular basis of how int6 regulates proteasome functioning will also be summarized.

Report Body

Task 1: Generate cell lines with reduced Int6 levels

I propose to generate siRNA that can knock down *int6* expression, the detection of which requires an anti-*int6* antibody (Fig. 1A). I thus raised a polyclonal Int6 antibody, which efficiently recognizes endogenous and ectopically expressed *int6* in many human cells including the MCF10A mammary epithelial cells. I was able to identify several siRNA sequences that can effectively knock down *int6* expression in both HeLa and MCF10A cells (Fig. 2). I have since moved on to build lentivirus expression vectors to express these siRNA sequences as shRNA to establish cell lines in which Int6 expression is stably knocked-down in MCF10A cells.

Task 2: Analyze genetic stability and mitotic abnormalities in engineered cell lines

I found that *int6* knockdown (*int6*$^-$) HeLa and MCF10A cells showed decreased viability (Fig. 3A-B, and data not shown). Furthermore, *int6*$^-$ cells frequently become multi-nucleated (Fig. 3C), and contain multi-polar spindle (Fig. 3D), suggesting that like in yeast, Int6 is important for proper chromosome segregation. To perform long-term genomic stability assay in MCF10A cells with stable knockdown of *int6*, we are building lentivirus expression vectors expressing shRNA to establish cell lines with stable knock-down of *int6*.

Task 3: Analyze proteasome functions in engineered cell lines

Our yeast data showed that Int6 bound the proteasome. I thus tested whether Int6 also binds the 26S proteasome in human cells. My current data showed that Int6 can intereact with at least one protasome subunit Rpt4 by co-immunoprecipitation assay (Fig. 4A). To test whether Int6 is important for proteasome functions in mammalian cells, we treated *int6*$^-$ HeLa cells with a proteasome inhibitor, MG132, and found that the *int6*$^-$ cells are more sensitive to this drug than cells treated with control siRNA (Fig. 4B), supporting the hypothesis that loss of *int6* can weaken the proteasome. The next step is to determine whether there is accumulatin of polyubiquitinated proteins in these *int6*$^-$ cells and then move on to examine MCF10A cells. To test whether *int6* inactivation weakened proteasome in human cells, I performed proteasome pull down assay to determine whether the presence of Int6 affects the protesome assembly. For this purpose, I generated a polyclonal antibody that recognizes Rpn5 in human cells to detect its presence in the pull down proteasome (Fig. 1B). Guided by this antibody, I found that in *int6*$^-$ cells, substantially less Rpn5 and Rpt4 co-precipitates in the assay (Fig. 4C). In conclusion, these data indicate that Int6 also binds the proteasome and regulates proteasome assembly and function in human cells. We are currently preparing a manuscipt to document these findings.

Task 4 and 5: Search for human high-copy suppressors of yeast *int6Δ* defects, as well as Int6-binding proteins.

Before conducting a screen using human cDNA, I performed a screen using *S. pombe* cDNA. From this screen, I isolated another proteasome subunit called Rpn7, which can rescue *int6*Δ defects when overexpressed. This protein,

like Int6 and Rpn5, also contains a PCI domain. With the isolation of Rpn7, I have together characterized three PCI proteins. I thus performed mutagenesis screen to identify conserved residues that is present in nearly all known PCI domains, in order to better understand the function of the PCI domain. I have identified such a Leucine residue, and a substitution of this residue to aspartic acid inactivated these proteins, leading to proteasome deficiencies and inefficient binding to proteasome subunits. Our bioinformatics analyses suggest that this leucine may influence the spatial arrangement either within the N-terminal tandem α-helical repeats or between these repeats and the more C-terminal winged-helix sub-domain. Disruption of such an arrangement in the PCI domain may substantially inactivate many PCI proteins and block their binding to other proteins. I have similarly mutated the corresponding residue in human Int6 and found that the resulting protein is inactive in yeast. A manuscript describing these findings has been submitted and is currently under review (see attached manuscript).

Additional Progress:

The 26S proteasome is structurally complex and found in numerous cell compartments. It is not known whether and how the proteasome moves in the cell and how proteasome mobility influences cell functions. Since Int6 may influence protasome localization in the cell, I performed a series of photobleaching experiments to determine whether proteasomes are mobile, and if so, how Int6 can influence their mobility. I chose to do this in the S. pombe model system because their endogenous proteins can be tagged with GFP with no loss of activity or structural abnormality, and S. pombe proteasome subunits are evolutionarily conserved in human. My data showed that proteasome subunits are similarly mobile in both the cytoplasm and the nucleus with a photobleaching recovery $\tau_{1/2}$ of just over 1 sec, after examining three subunits (Fig. 5). Deletion of *yin6* as well as *rpn5* substantially increases the mobility of proteasome subunits, presumably due to loss of protesome integrity (Fig. 6). The high mobility of the proteasome is at least partly actin-dependent, and actin defects the mobility, as well as activity, of the proteasome (data not shown). A manuscript describing these findings is currently in preparation, and will be submitted in one month.

Key Research Accomplishments

1. I have generated and confirmed anti-human Int6 and Rpn5 antibodies in human mammary epithelial cells (Fig. 1), and I have generated siRNA sequence that can transiently knock-down *int6* expression in both HeLa cells and MCF10A cells. (Fig. 2)

2. I found that knock down of int6 causes growth defects and mitotic defects in human mammary epithelial cells (Fig. 3).

3. I found that *int6* can co-immunoprecipitate proteasome subunit Rpt4 in human mammary epithelial cells (Fig. 4A). Knockdown of *int6* causes weakened proteasome functioning (Fig. 4B), and also affects proteasome integrity, as shown by co-immunoprecipitation (Fig. 4C).

4. I identified a conserved leucine residue in the PCI domain, which is essential for proper localization, assembly and functioning of both Yin6 and proteasome subunits Rpn7 and Rpn5 in fission yeast cells. (See attached manuscript)

5. I found that proteasome is highly mobile in *S. pombe* cells (Fig. 5). Int6 affects proteasome mobility by maintaining proper proteasome integrity (Fig. 6). The mobility is at least partly dependent on F-actin, and this actin-dependent mobility is important in regulating proteasome functioning.

Reportable Outcomes

1. Polyclonal anti Int6 and Rpn5 antibodies

2. siRNA for reducing Int6 expression in human mammary epithelial MCF10A cells.

3. Posters presented in meetings:

3.1. Annual Graduate Student Research Symposium, Baylor college of Medicine

Sha Z. and Chang EC., Regulation of proteasome nuclear import and assembly by Int6. The 16th Annual Symposium, October, 2004.

Sha Z., Suo J. and Chang EC., Regulation of proteasome nuclear transport and assembly by Int6. The 17th Annual Symposium, October, 2005.

Sha Z. and Chang EC., Regulation of proteasome dynamics and assembly by Int6. The 18th Annual Symposium, Nov, 2006.

3.2. Annual Department of Molecular and Cellular Biology Graduate Student Symposium

Sha Z., Cabrera R., and Chang EC., Regulation of proteasome nuclear import and assembly by Int6. The 26th Annual Symposium. April, 2004.

Sha Z., Suo J. and Chang EC., Regulation of proteasome transport and assembly by Int6. The 27th Annual Symposium. April, 2005.

Sha Z. and Chang EC., Regulation of proteasome dynamics and assembly by Int6. The 28th Annual Symposium. April, 2006

3.3. Sha Z., Cabrera R., and Chang EC., Regulation of proteasome nuclear import and assembly by Int6. The 2004 ASBMB/IUBMB Annual Conference. Boston, MA. June, 2004.

3.4. Sha Z., Suo J. and Chang EC., Regulation of proteasome transport and assembly by Int6., The 4th Era of Hope meeting for the Department of Defense (DOD) Breast Cancer Research Program (BCRP), Philadelphia, PA, June, 2005

3.5. Sha Z. and Chang EC., Regulation of proteasome nuclear transport and assembly by Int6. The 45th American Society for Cell Biology Annual Meeting, San Francisco, CA, December, 2005

3.6. Sha Z. and Chang EC., Regulation of proteasome nuclear transport and assembly by Int6. The 3rd "Ubiquitin, Ubiquitin-Like Proteins And Cancer" International Conference, MD Anderson Cancer Center, Houston, TX, February, 2006

3.7. Sha Z. and Chang EC., Regulation of proteasome dynamics and assembly by Int6. ZOMES-IV International Conference. New Haven, CT, June, 2006

3.8. Sha Z. and Chang EC., Regulation of proteasome dynamics and assembly by Int6. The 46th American Society for Cell Biology Annual Meeting, San Diego, CA, December, 2006

3.9. Sha Z., Yen HC., and Chang EC., Dynamics of the 26S proteasome in Schizosaccharomyces pombe. The Ubiquitin and Signaling (B4-2007) conference, Big Sky, MT, February, 2007.

3.10. Chang EC., **Sha Z.,** and Yen HC., Characterization of a *Schizosaccharomyces pombe* proteasome subunit Rpn7, which contains a PCI domain that is critical for binding other proteasome subunits. The Ubiquitin and Signaling (B4-2007) conference, Big Sky, MT, February, 2007.

4. Oral Presentations:

4.1. Annual Breast Cancer Center Retreat, Baylor College of Medicine

Sha Z., Suo J. and Chang EC., Regulation of proteasome transport and assembly by Int6. The 1st Annual Retreat. September, 2005.
Sha Z. and Chang EC., Regulation of proteasome dynamics and assembly by Int6. The 2nd Annual Retreat. October, 2006

4.2. Breast Cancer Center Data Review, Baylor College of Medicine

Sha, Z. and Chang, EC. Regulation of proteasome nuclear import and assembly by Int6. Jun, 2003.

Sha, Z. and Chang, EC. Regulation of proteasome nuclear transport and assembly by Int6. May, 2004.

Sha, Z. and Chang, EC. Regulation of proteasome transport and assembly by Int6. January, 2005.

Sha, Z. and Chang, EC. Regulation of proteasome transport and assembly by Int6. Dec, 2005.

Sha, Z. and Chang, EC. Regulation of proteasome dynamics and assembly by Int6. July, 2006.

4.3. Sha, Z. and Chang, EC. Regulation of proteasome nuclear transport and assembly by Int6. Society of Chinese BioScientists in America annual symposium. Houston, TX. April, 2005.

4.4. Sha, Z. and Chang, EC. Regulation of proteasome nuclear transport and assembly by Int6. the 2nd East Coast Regional Fission Yeast Meeting, Miami, TX. April, 2005.

4.5. Sha Z., Yen HC., Cabrera R., Scheel, H., Hoffman, K., and Chang EC., Regulation of proteasome dynamics and assembly by Int6. M&CB - R&D Workshop Series. Jan., 2007.

4.6. Sha Z., Yen HC., Cabrera R., and Chang EC., Regulation of proteasome dynamics and assembly by Int6. The 29th Annual Department of Molecular and Cellular Biology Graduate Student Symposium. April, 2007

5. Publications:

Zhe Sha, Hsueh-Chi S. Yen, Jinfeng Suo, Hartmut Scheel, Kay Hofmann, and Eric C. Chang, Characterization of a *Schizosaccharomyces pombe* proteasome subunit Rpn7 containing a PCI domain that is critical for binding other proteasome subunits, Submitted and under review, 2007.

Conclusions

The main goal of my study is to test the hypothesis, that a key conserved function of *int6* is to regulate the 26S proteasome, thus ensure genetic stability. In summary, I have productively accomplished nearly all the objectives for this project. I found that Int6 also bound the proteasome, and positively regulated proteasome assembly and functioning in human cells. As a result, inactivation of *int6* in human cells leads to mitotic abnormalities. These functions of *int6* require its PCI domain, since mutation of a Leucine residue in the PCI domain inactivates Int6 and abolishes its binding to the proteasome. Since genetic instability is an important risk factor for tumorigenesis, better understanding of these functions of *int6* can bring insight into developing effective strategies for cancer prevention and treatment. Future studies will focus on testing the direct binding between *int6* and the proteasome, testing the regulation of proteasome-dependent degradation of mitotic regulators by *int6*, and carrying out a screen to isolate more human *int6* interacting proteins.

Through the course of these studies, I better appreciate the values of using fission yeast as a model system to carry out mechanistic studies that can guide research in human. Moreover, I am very excited to receive the training to directly test these evolutionarily conserved functions in human cells. As a member of the breast center, I met and cooperated with experts in both areas to broaden my sight of viewing science. These rewarding experiences will better equip me to be a breast cancer researcher.

References

1. Tekmal, R.R. and N. Keshava, *Role of MMTV integration locus cellular genes in breast cancer.* Front Biosci, 1997. **2**: p. d519-26.
2. Miyazaki, S., et al., *The chromosome location of the human homolog of the mouse mammary tumor-associated gene INT6 and its status in human breast carcinomas.* Genomics, 1997. **46**(1): p. 155-8.
3. Marchetti, A., et al., *Reduced expression of INT-6/eIF3-p48 in human tumors.* Int J Oncol, 2001. **18**(1): p. 175-9.
4. Venkitaraman, A.R., *Cancer susceptibility and the functions of BRCA1 and BRCA2.* Cell, 2002. **108**(2): p. 171-82.
5. Yen, H.C. and E.C. Chang, *Yin6, a fission yeast Int6 homolog, complexes with Moe1 and plays a role in chromosome segregation.* Proc Natl Acad Sci U S A, 2000. **97**(26): p. 14370-5.
6. Yen, H.C., C. Gordon, and E.C. Chang, *Schizosaccharomyces pombe Int6 and Ras homologs regulate cell division and mitotic fidelity via the proteasome.* Cell, 2003. **112**(2): p. 207-17.
7. Yen, H.C. and E.C. Chang, *INT6--a link between the proteasome and tumorigenesis.* Cell Cycle, 2003. **2**(2): p. 81-3.

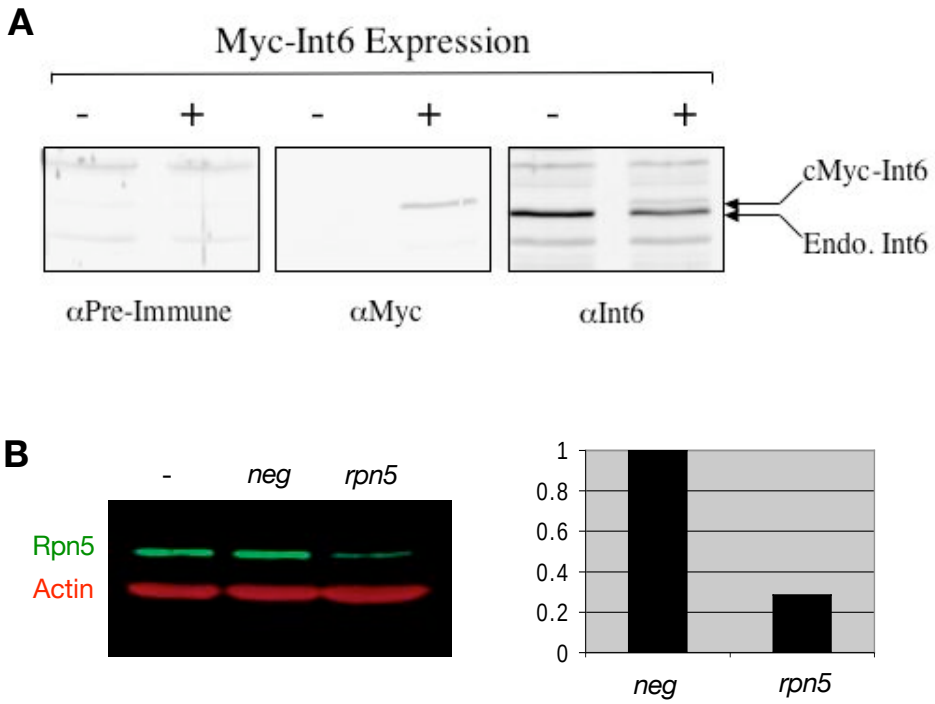

Figure 1: Testing of anti-Int6 and anti-Rpn5 antibodies

A. Detection of Int6 in MCF10A cells by α-Int6 antibody Int6-N1. MCF10A cells were transfected by a vector expressing Myc-Int6 or by an empty vector. Cell lysate was subject to Western blotting with α-Myc antibody or α-Int6 antibody Int6-N1. Int6-N1 recognizes both the endogenous Int6 and the ectopically expressed Myc-Int6.

B. Detection of Rpn5 in MCF10A cells by α-Rpn5 antibody Rpn5-N2. MCF10A cells were transfected with either an α-*rpn5* siRNA, or a nonspecific siRNA as a negative control (*neg*). Cell lysate was subject to Western blotting with α-Actin antibody (red) as a loading control, or α-Rpn5 antibody Rpn5-N2 (green). Rpn5-N2 recognizes the endogenous Rpn5 protein, which was specifically knocked down by α-*rpn5* siRNA. Quantification of relative amount of protein from the Western blot is shown on the left.

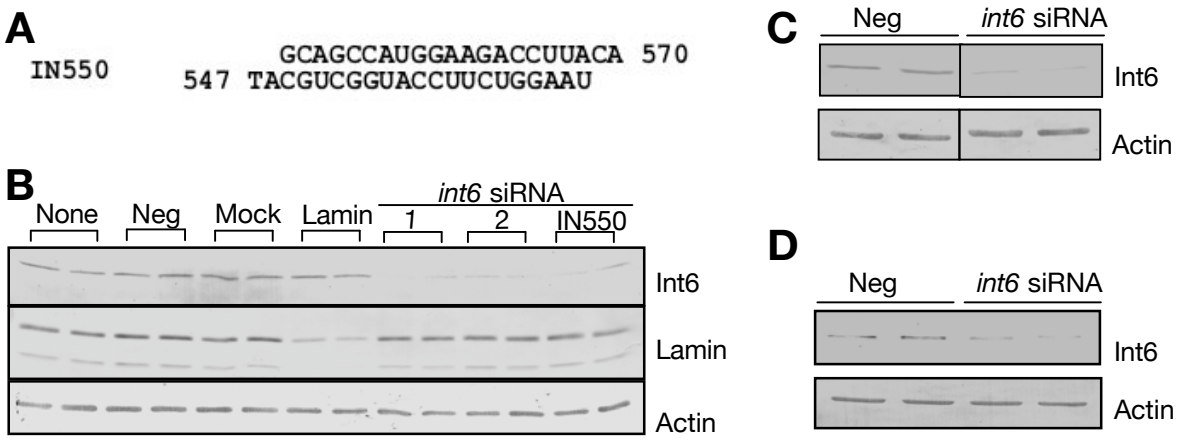

Figure 2: Suppression of Int6 levels in HeLa Cells and human mammary epithelial cells by synthetic siRNA

(A) Sequence of siRNA (I550) designed for suppressing Int6 protein levels in human mammary epithelial cells. (B) Anti-Int6 western blotting (top) to confirm successful suppression of Int6 level in HeLa cells transiently transfected with indicated siRNA. Non-specific siRNA and anti-Lamin siRNA were included as negative and positive controls, respectively, and anti-lamin (bottom) western blotting was included as loading control and to confirm the effect of the siRNA-mediated suppression of gene expression. Cell lysate was prepared in duplication. (C) and (D) Anti-Int6 western blotting to confirm successful suppression of Int6 level in MCF10A (C) or MCF10AT (D) cells transiently transfected with indicated siRNA. β-actin was included as loading control.

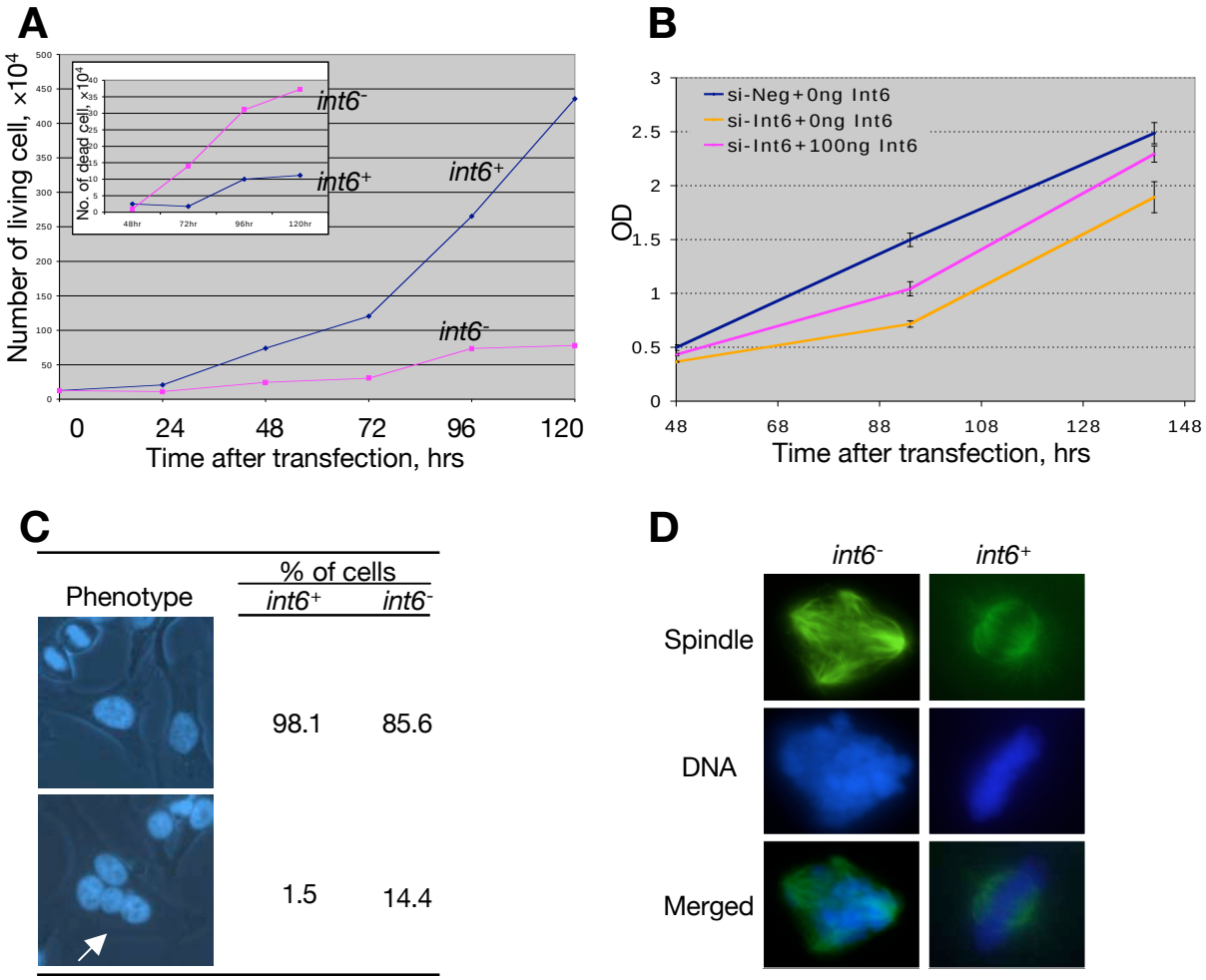

Figure 3: *int6* knockdown causes growth defects and abnormal mitosis.
(A) HeLa cells with transiently transfected control (*int6*$^{+}$) or anti *int6* (*int6*$^{-}$) siRNA were cultured for 5 days after transfection, and number of living cells and dead cells (insert) were counted and plotted over time. (B). HeLa cells transiently transfected with indicated siRNA plus or minus 100ng Int6 expression vectors were cultured as in (A), and cell number was quantified by measuring OD and plotted over time. (C). HeLa cells in which Int6 expression has been reduced by siRNA were stained to reveal DNA, and cells with multiple nuclei (arrow) can be readily detected. Percentage of normal cells or cells with multiple nuclei was quantified and compared. (D). Same cells as in (C) were stained to reveal mitotic spindle (Green) and DNA (Blue). Representative mitotic cell with multi-polar spindle and mis-alligned chromosome was shown and compared to *int6*$^{+}$ control cells.

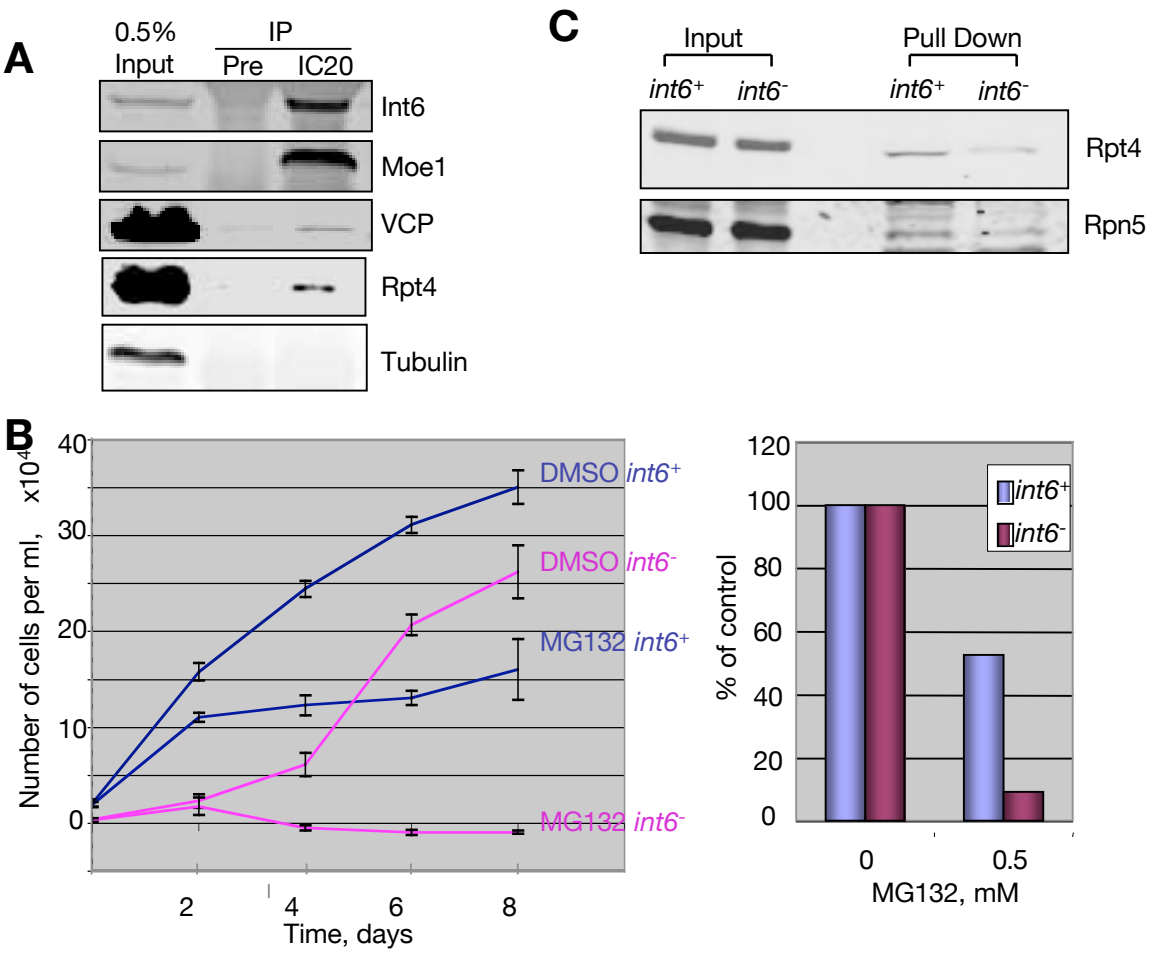

Figure 4: Int6 physically and functionally associates with the proteasome in human cells
(A). Cell lysate from MCF7 cells were immunoprecipitated with anti-Int6 (IC20) antibody or control pre-immune serum (Pre). The co-immunoprecipitated proteins were analyzed by Western blots using antibodies specific for proteins as indicated on the right. (B) HeLa cells with transiently transfected control (*int6*$^{+}$) or anti *int6* (*int6*$^{-}$) siRNA were cultured for 8 days in medium containing MG132 or DMSO, and number of cells were counted and plotted over time (Left). Percentage survival was calculated by comparing cell number in MG132 treated group to control group on the 4th day (Right) (C). Cell lysate from *int6*$^{+}$ or *int6*$^{-}$ HeLa cells were subjected to pull down with proteasome purification beads (Calbiochem. Cat#539176). The pull down samples were analyzed by Western blots using antibodies specific for proteins as indicated on the right.

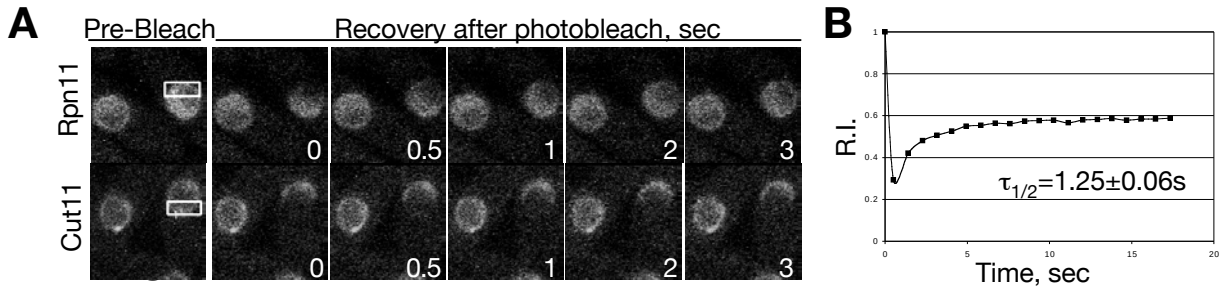

C

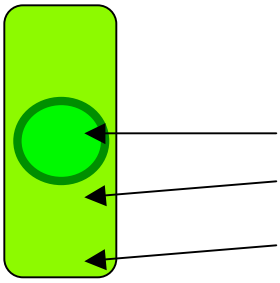

Region of cell	$\tau_{1/2}$(sec) of Pro. Sub.		
	Rpn11	Rpn7	α4
Nuclear	1.31±0.03	1.46±0.05	1.35±0.05
Peri-Nuclear	1.35±0.05	1.33±0.06	1.34±0.05
Cell Tip	1.58±0.06	1.46±0.05	1.23±0.04

Figure 5: The 26S proteasome subunits mobility in *S. pombe* cells, as measured by FRAP: (A) FRAP was performed on cells whose endogenous Rpn11 or Cut11 was tagged by GFP via homologous recombination. The rectangles over the un-bleached cells mark the area of photobleaching. Images of cells after photobleaching were captured with the pin-hole set to the maximal level to increase sensitivity as yeast cells are small and the GFP signal dim. Note that a single pulse of laser to one area in the nucleus led to such a rapid decline of fluorescence in the entire nucleus that a full fluorescence recovery was not observed. (B) The fluorescence in the region of interest (ROI) at each time point was corrected for background autofluorescence and for spontaneous photobleaching (by comparing fluorescence signals from neighboring unbleached cells). "R. I." (relative fluorescence intensity) is the corrected fluorescence intensity in the ROI relative to that prior to photobleaching. Approximately 25 cells were used to yield statistically reliable $\tau_{1/2}$ values (Ave±SEM). To present these data in a graph, we plotted the average R.I. of each time point. (B) The $\tau_{1/2}$ values (Ave±SEM) of three proteasome subunits in three regions of the cell were similarly measured as in (A) and tabulated.

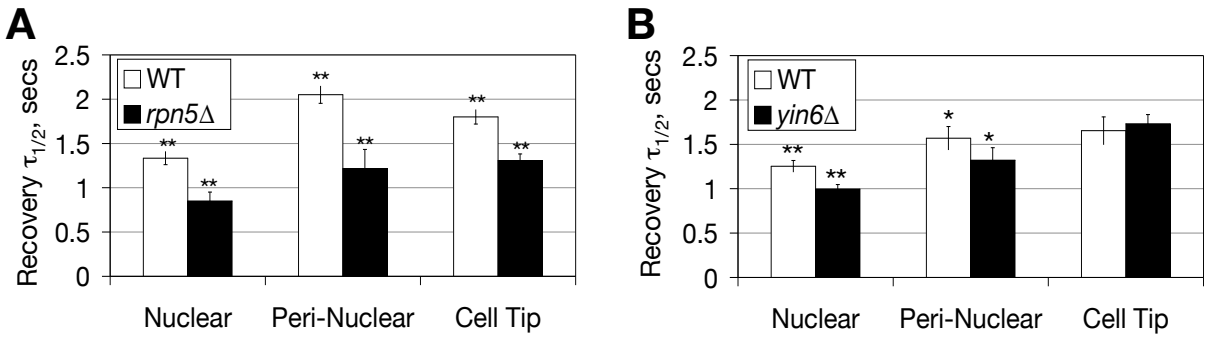

Figure 6: Disruption of proteasome assembly increases apparent subunit mobility:
(A) FRAP experiments similar to that in Fig. 4 was carried out in *rpn5*Δ cells (strain 11GFP5Δ), as well as the parental wild type strain (strain 11GFP), and the $\tau_{1/2}$ values in different cell compartments between the two strains were graphed. (B) The same experiment was performed in *yin6*Δ cells carrying Rpn11-GFP (strain 11GFPY6K). ** $p<0.01$; *$p<0.05$.

Characterization of the *Schizosaccharomyces pombe* proteasome subunit Rpn7– a PCI domain leucine critical for binding other proteasome subunits.

Running title: A leucine critical for PCI domain functions

Zhe Sha*, Hsueh-Chi S. Yen*, Hartmut Scheel[¶], Kay Hofmann[¶], and Eric C. Chang*[§]

*Baylor College of Medicine

1 Baylor Plaza, BCM 600

Department of Molecular and Cell Biology

The Breast Center

Houston, TX 77030

USA

[¶]Miltenyi Biotec GmbH

MACSmolecular Business Unit

Bioinformatics Department

Nattermannallee 1

D-50829 Cologne

Germany

[§]Corresponding author: 713-798-3519 (P) /713-798-1462 (F)/echang1@bcm.edu

Proper assembly of the 26S proteasome is required to efficiently degrade polyubiqitinated proteins. Many proteasome subunits contain the PCI domain, thus raising the possibility that the PCI domain may play a role in mediating proteasome assembly. We have previously characterized the PCI protein Yin6, a fission yeast ortholog of the mammalian Int6 that has been implicated in breast oncogenesis, and demonstrated that it binds and regulates the assembly of the proteasome. In this study, we isolated another PCI protein, Rpn7, as a high copy suppressor that rescued the proteasome defects in *yin6* null *(yin6*Δ) cells. Rpn7 bound the proteasome apparently via Rpn9, and its colocalization with other proteasome subunits was disrupted by *yin6*Δ or *rpn5*Δ. Furthermore, inactivating Rpn7 induced accumulation of polyubiquitinated proteins and abnormal mitosis. These data indicate that Rpn7 is a proteasome subunit and that its assembly and/or colocalization with the proteasome require Rpn5 and Yin6. To determine how the PCI domain regulates proteasome assembly, we performed protein sequence alignment to identify a conserved leucine residue that is present in nearly all known PCI domains. Replacing it with aspartate in Rpn7, Yin6, and Rpn5 inactivated these proteins, leading to proteasome deficiencies and inefficient binding to proteasome subunits. Our bioinformatics analyses suggest that this leucine may influence the spatial arrangement either within the N-terminal tandem α-helical repeats or between these repeats and the more C-terminal winged-helix sub-domain. Disruption of such an arrangement in the PCI domain may substantially inactivate many PCI proteins and block their binding to other proteins.**

The 26S-proteasome contains a 20S catalytic core, which has a cylindrical shape, and on its own is capable of degrading small peptides (1). However, eukaryotic proteins that are designated for degradation are frequently marked by poly-ubiquitination, which apparently increases the bulk of the protein to make it difficult to enter the small catalytic chamber. To degrade polyubiquitinated proteins, two 19S regulatory particles are needed, and they cap the two ends of the 20S catalytic core to produce the 26S proteasome. In order to understand how the 26S proteasome efficiently and selectively degrades proteins, it is critical to ascertain how a 26S proteasome is properly assembled.

A 19S regulatory particle can be further divided into a lid and a base subcomplex, each of which contains approximately eight subunits. Intriguingly, more than half of the lid subunits contain a PCI (Proteasome-COP9-Initiation factor)[1] domain, thus named because it is frequently found in three protein complexes, which, beside the proteasome, include the COP9/signalosome and e-IF3 translation initiation complex (2,3). The common presence of PCI domains in these protein complexes supports a model in which the PCI domain can play a role in assembling subunits within or even between these complexes (4).

The PCI domains remain structurally poorly defined. So far the only relevant crystal structure of the PCI domain is that of human e-IF3k (5), as this protein is a more distant member in the PCI family (6). In the structural study of Wei et al,

the authors have concluded that the PCI domain in e-IF3k actually contains two subdomains, and this two-subdomain architecture is probably also true for more typical PCI domains. The e-IF3k PCI N-terminal sub-domain was termed HAM (HEAT analogous motif; Fig. 1A, Green) because it resembles the HEAT helical repeats found in numerous proteins whose main roles appear to be binding and assembling other proteins. In a previous bioinformatic analysis of PCI architecture (6), we predicted that the N-terminal subdomain of typical PCI domains most likely resembles the Tetratrico Peptide Repeat (TPR), which consists of pairs of α-helices that are oriented in an anti-parallel manner. Compared to the HEAT repeats, the functionally similar TPR has a slightly different arrangement of helices.

The C-terminal sub-domain in the e-IF3k PCI was determined to be a winged helix (WH, Fig. 1B, yellow)(5), which is also likely to be conserved in the other PCI domains. Together with the TPR/HEAT repeat subdomain, these two subdomains create two large surfaces, one of which is concave and one of which is convex, resulting in an ear-like shape. The presence of these two large surfaces may allow a PCI protein to provide ample binding areas for many proteins. However, no detailed structure-function analyses have yet been performed to investigate whether the presence of these two subdomains is physiologically relevant.

Our lab has characterized a PCI protein called Yin6 in the fission yeast *Schizosaccharomyces pombe (7).* Yin6 is the *S. pombe* ortholog of the mammalian Int6 protein that has been implicated in breast tumorigenesis (8-10), although its molecular functions are poorly defined. Int6 is also known as e-IF3e because it was found to co-purify with the e-IF3 complex (11). We and others have shown that Yin6 is not essential for global translation initiation (12). By contrast, we have found that a major evolutionarily conserved function of Yin6 is to regulate the 26S proteasome by preferentially binding and controlling the localization and/or assembly of a PCI proteasome lid subunit, Rpn5 (13,14). That is, in wild type *S. pombe* cells, the proteasome is concentrated in the inner layer of the nuclear membrane. By contrast, in *yin6* null (*yin6*Δ) cells as well as *rpn5*Δ cells, the proteasome appears more diffuse in the cell, as measured by microscopy, and lacks many subunits, as revealed by affinity pull-down.

To better define the role of Yin6, we carried out a high-copy suppressor screen seeking *S. pombe* genes that when overexpressed rescued the cold-dependent growth defect of *yin6*Δ cells. In support of the model that Yin6 regulates the proteasome, we report herein the isolation of another PCI proteasome subunit, Rpn7, from the screen. Since together with Yin6 and Rpn5, we now have three well-characterized PCI proteins, we performed a structure-function analysis to identify amino acid resides in the PCI domain that may be important for the function of many PCI proteins. We have thus identified a leucine (Leu) residue that is critical for the functions of these three proteins. Bioinformatics analysis showed that this Leu appears to reside in a region that is in close proximity to both the TPR-like and the WH sub-domains. The hydrophobic interactions provided by the identified Leu may influence how each of these two sub-domains folds, or how they are arranged relative to one another, or both. Collectively, these data suggest that maintaining proper conformation of these two sub-domains is indeed important for the function of many PCI proteins.

EXPERIMENTAL PROCEDURES

Strains and growth conditions

The parental wild-type *S. pombe* strain used in this paper is SP870 (*h*^{90}*, ade6-M210, leu1-32, ura4-D18*). The *yin6*Δ*, rpn5*Δ, and *pus1/rpn10-PA* strains were as described (13,14). Cells were grown in either yeast extract medium (YEAU) or synthetic minimal medium (MM) with appropriate supplements. To test for canavanine sensitivities, stock solutions of canavanine sulfate (50 mg/ml in water) were prepared and added to media after autoclaving. We carried out all the experiments with cells pregrown to early logarithmic phase (2-5×10^6 cells/ml). For growth experiments on plates, cells were serially diluted 1:5.

Highcopy suppressor screen

The YIN6K strain (*yin6::kan*^{R}, (7)) was transformed with a cDNA library whose cDNA clones are carried by the pREP3 vector that contains a thiamine-repressible *nmt1* promoter (15). Transformed cells were incubated at 20ºC for 6 weeks, and plasmid DNA was isolated from colonies that emerged. These cDNA clones were re-tested with a fresh batch of YIN6K cells, and those that failed to rescue the growth defects were discarded. The final cDNA clones were sequenced using two primers: 5'-CAATCTCATTCTCACTTTCTGAC-3' and 5'-TTGAATGGGCTTCCATAGTTTG-3'. The former anneals in the *nmt1* promoter, while the latter anneals to the *nmt1* terminator. The obtained sequences were submitted to the BLAST server at the *S. pombe* sequencing project at Sanger Institution (16). In addition to *yin6,* which was isolated 6 times, two identical *rpn7* clones (SPBC582.07c) were isolated. These two clones do not have the coding sequence for the first 8 amino acids. The 12th amino acid in the Rpn7 protein is a methionine; therefore, we assumed that protein expression from these two plasmids starts from this second methionine. All the Rpn7 vectors described in this study contain the full-length *rpn7* gene, however. This screen has also isolated other genes, but they will be described elsewhere in the future.

Plasmid constructions:

The construction of pREP1YIN6, pGADYIN6, pLBDMOE1, pGADRPN9, and pLBDRPN5 was as described (7,13,14). A *Bam*H1 *rpn7* cDNA fragment was amplified by PCR from the cosmid SPBC582 (16) and subcloned into pVJL11 (17), pREP1, pREP41, pREP41GFP to create pLBDRPN7, pREP1RPN7, pREP41RPN7, and pREPGFPRPN7. All PCR products in this study have been verified by sequencing to make sure that there is no mutation altering the coding sequence. In a separate project, we (Xin-rong Fu and Eric Chang, unpublished) have constructed an expression vector that was derived from pNR210gck (18), and uses the *cdc42* promoter to express fusion proteins that are N-terminally tagged by a monomeric form of RFP (mcRFP) called mCherry (19). To tag Rpn7 with this RFP, the *rpn7* cDNA was modified by PCR to contain *SalI* and *SphI* sites for cloning, and the resulting vector is named pMCRPN7. All site-directed mutatgenesis was performed by the QuickChange Kit (Stratagene). pAL1YIN6g contains the genomic version of the wild type *yin6* gene in a high copy Leu+ vector pAL1 (7). The coding sequence of wild type *yin6* in this vector was replaced with the mutated ones, and the

final vector expressing Yin6L332D was named pYIN6LD. The wild type human *int6* in pHAHINT6 (7) and the wild type *yin6* in pHAYIN6 (7) were similarly mutated to create pHAHINT6LD and pHAYIN6LD. The mutant *rpn5* and *rpn7* gene products were also subcloned into pVJL11, pREP41, and pREP41GFP to create pLBDRPN5LD, pLBDRPN7LD, and pREPGFPRPN7LD.

Strain constructions

*rpn7*Δ/+ heterozygous diploid cells were created by homologous recombination of an *rpn7::ura4* fragment amplified from the *KS-ura4* plasmid as described (20), and this was also the method that we first chose to tag Rpn7 with GFP at the C-terminus by the pFA6a-GFP(S65T)-kanMX6 plasmid. This approach of tagging does not deliberatively create an amino acid spacer between Rpn7 and GFP, and the resulting strain displayed a temperature-sensitive growth defect. We thus named this strain RPN7TS. To properly perform gene tagging using PCR and homologous recombination, we used a different plasmid, pYM27, as described by another group (21). This approach creates a poly-AG spacer between the gene of interest and GFP. Proper tagging was confirmed by Western blots (Supplemental figure S1). The resulting strain was named RPN7-GFP. The same method was used to tag Rpn7 with GFP in *yin6*Δ, *rpn5*Δ, and *pus1/rpn10-PA* cells to create strain Y6AR7GFP, R5AR7GFP, and R10PAR7GFP. We used similar method to tag Rpn11 and α4 and the resulting strains were named RPN11GFP and A4GFP.

The pYIN6LD vector was linearized and allowed to integrate to the chromosome of *yin6*Δ cells (strain YIN6K, (7)) to create strain YIN6LD such that the only copy of *yin6* in this strain is the mutant version. In parallel, the same mutant *yin6* was integrated into a wild type strain to make sure that it did not induce an *yin6*Δ-like phenotype (data not shown). Other *yin6* mutant genes were examined similarly. *S. pombe* contains two copies of *rpn5* genes, *rpn5a* and *rpn5b* that encode an identical protein (14). The expression of these two loci is tightly regulated such that when one of them is deleted, the expression of the second locus will increase to maintain the same level of total Rpn5 protein. Site-directed mutagenesis was carried out to similarly mutate the *rpn5* coding sequence in pBSRPN5-HAKan^R (14) to create pBSR5LD-HAKan^R. This plasmid was digested by *XhoI* and *SmaI* to release a fragment containing *rpn5* and this fragment was used to transform a *rpn5b*Δ strain (RPN5bA, ref 14). After homologous recombination its *rpn5a* locus was replaced by *rpn5L316L-HAKan^R*. We named the resulting strain RPN5LD.

Fluorescence microscopy

The general procedures for 4',6-diamidino-2-phenylindole (DAPI) staining were as described (22). Samples were examined via a UPlanFI 100×/1.30 Oil objective on an Olympus BX61 microscope, and the images were captured by a Q-Imaging Retiga camera. Deconvolution of images (Nearest Neighbor) was performed using Slide Book 4.0. software. For protein colocalization study, images in each focal plan were examined to confirm colocalization.

26S proteasome pull-down

Approximately 30 OD units (~ 3×10^8) of cells were lysed in ice-cold 26S-binding buffer (25 mM Tris, 50 mM NaCl, 10 mM $MgCl_2$, 1 mM DTT, 5 mM ATP, 0.1% Triton X-100, 20% glycerol, pH 7.0-7.4).

Total crude lysates were centrifuged twice at 20,800×g for 20 min. Supernatants with the same amount of protein were incubated with either 50 µl IgG Sepharose (Invitrogen) or Protein A Sepharose control (Sigma) overnight at 4°C. After 8 washes in the 26S-binding buffer, beads were incubated with the TEV protease (Invitrogen) twice for 1 hr at 30°C to release the 26S proteasome. Eluted proteins were analyzed by SDS-PAGE and Western blots. Antibodies against Mts4/Rpn1 were as described (13) and used at 1:1,000 dilution. Antibodies against proteasome 20S core α subunits (MCP231, 1:1,000) and GFP (1:1,000) were from BIOMOL and Clontech. The existing antibody against the α core does not recognize the α4 subunit so we generated a polyclonal rabbit antibody using CIVKEIQDEKEAEAARKKGR as a peptide antigen. The confirmation of this antibody (1: 2,000) is shown in supplemental figure S2.

Yeast two-hybrid assay

The yeast two-hybrid assay was performed as described (17). Briefly, the reporter strain was L40, which carries the reporter gene cassettes lexA-HIS3 lexA-lacZ. The β-galactosidase activity was assayed by a color filter assay using X-Gal (5-bromo-4-chloro-3-indolyl-β-D-galactoside) as substrate, while HIS3 expression was assayed by plating cells in medium lacking histidine.

Detection of polyubiquitinated proteins

To detect ubiquitinated proteins, cells were broken by glass beads in PBS (pH 7.4). Total crude extracts containing equal amounts of proteins were analyzed by immunoblotting with an ubiquitin antibody (1:100, from Sigma).

RESULTS

Isolation of Rpn7 as a high copy suppressor that rescues yin6Δ phenotypes

The cDNA encoding a putative proteasome subunit in the lid of the 19S cap particle was isolated twice in a genetic screen in which we sought *S. pombe* cDNAs that when overexpressed rescued the cold-dependent growth defects of *yin6*Δ cells (Fig. 2A). We named it Rpn7 based on its sequence homology to other Rpn7 proteins. Canavanine is an arginine analog; cells defective in the proteasome, such as *yin6*Δ cells, are hypersensitive to this drug. We found that overexpressing Rpn7 also rescued canavanine hypersensitivity of *yin6*Δ cells, a result that is consistent with the possibility that Rpn7 is a proteasome subunit (Fig. 2B).

Rpn7 is essential for proteasome functioning

To determine whether *rpn7* encodes an essential proteasome subunit, we deleted and replaced it with the *ura4* selectable marker via homologous recombination in a diploid cell, and the deletion (*rpn7::ura4*) was confirmed by PCR. Tetrad analysis of its meiotic products showed that only 2 out of the four spores in a given tetrad formed colonies (Fig. 3A) and they were all auxotrophic for uracil (Ura^-, data not shown), indicating that a single essential gene had been replaced by *ura4*. Finally we transformed the heterozygous *rpn7*Δ/+ diploid cells with a plasmid expressing the *rpn7* cDNA. By random spore analysis, we were able to easily identify cells that were uracil prototrophic (Ura^+; data not shown), indicating that the expression of *rpn7* cDNA rescued the lethality of *rpn7*Δ cells, as expected.

These data collectively indicate that *rpn7* is a gene essential for viability.

During the course of an unsuccessful gene tagging experiment, we found that Rpn7 that was C-terminally tagged with GFP without a proper amino acid spacer induced growth defects that were temperature sensitive (ts), and this ts phenotype could be rescued by overexpressing *rpn7*. These data indicate that the ts growth defect is caused by loss of Rpn7 function (data not shown). We thus used this strain, called RPN7TS, to more efficiently analyze Rpn7 functions and its relationship to the proteasome, and the *rpn7* allele in this strain is called $rpn7^{ts}$. In Fig. 3B, we show that at even semi-permissive temperature, abnormal mitotic RPN7TS cells accumulated. In particular, cells that had apparently undergone abnormal chromosome segregation were frequently observed, which is consistent with the fact that sister-chromatid separation during anaphase is a key event regulated by the proteasome. To determine whether such a phenotype can be similarly detected in *rpn7*Δ cells, we sporulated diploid cells heterozygous for *rpn7::ura4* in medium lacking uracil, so that only *rpn7*Δ (*rpn7::ura4*) cells could grow. We found that all germinated cells divided just a few times and displayed the same mitotic abnormalities as seen in RPN7TS cells (data not shown). We conclude that the $rpn7^{ts}$ allele recapitulates the deficiencies in *rpn7*Δ cells. Cells defective in the proteasome are expected to show hypersensitivity to canavanine and to accumulate polyubiquitinated proteins, and indeed, both phenotypes were readily detected in RPN7TS cells (Fig. 3 C and D, respectively). These data demonstrated that Rpn7 is critical for proper proteasome functions.

Rpn7 associates with the proteasome and preferentially binds Rpn9

Having concluded that Rpn7 is critical for proteasome functions, we went on to determine whether Rpn7 binds the proteasome. We used a different tagging strategy to introduce a spacer between Rpn7 and GFP (Experimental Procedures). In the resulting strain, Rpn7-GFP is expressed from its authentic chromosomal locus by its own promoter. This strain showed no detectable growth defects in a wide range of temperatures and was not hypersensitive to canavanine (data not shown), indicating that unlike the Rpn7-GFP in the RPN7TS strain, this Rpn7-GFP is fully functional. In Fig 4A, we show that Rpn7-GFP clearly concentrated at the nuclear envelope. To determine whether Rpn7 colocalized with other proteasome subunits by deconvolution microscopy, we tagged Rpn7 with a monomeric RFP (mcRFP) and tagged two proteasome subunits (Rpn11 and α4) with GFP and found that indeed they colocalize (Fig 4A and data not shown). By contrast, Rpn7-GFP in the RPN7TS strain mislocalized in the nucleoplasm (Supplemental Fig. S2). Furthermore, like other proteasome subunits (14), Rpn7-GFP is mislocalized in *rpn5*Δ and *yin6*Δ cells (Fig. 4B). These data together strongly suggest that, like other proteasome subunits, Rpn7 is concentrated at the nuclear periphery and its mislocalization weakens the proteasome.

To biochemically examine whether Rpn7 is indeed part of the entire proteasome, we performed a proteasome affinity pull-down and detected the presence of Rpn7 with other proteasome subunits (Fig. 4C). Finally we employed the yeast two-hybrid assay to ascertain to which available proteasome subunits Rpn7 binds preferentially. Our data showed that Rpn7 bound Rpn9 (Fig. 4D), but not Rpn5,

Rpn10/Pus1, Rpn1/Mts4, Rpt1, Rpt2/Mts2, Rpt5, or Rpt6. We conclude from these data that Rpn7 is a proteasome subunit and is essential for viability and normal mitosis.

Identification of an essential leucine residue in the PCI domain of many proteins

Rpn7, as well as Yin6 and many proteasome subunits in the lid, contains the PCI domain; however, the exact function of the PCI domain remains elusive. The truncated Int6 identified in the mouse mammary tumors lacks the entire PCI domain (8), and we have found that these truncated human Int6 proteins are not functional in *S. pombe* (7,13). These results suggest that the PCI domain is critical for the function of Int6. Since the MMTV insertion in *int6* removes nearly 1/3 of the protein, which may broadly and severely affect the function of any protein, we conducted a structure-function analysis to identify single essential amino acid residues in the PCI domain and then analyze the function of the resulting proteins.

We first focused on amino acid residues that are highly conserved among many PCI proteins, as illustrated in our original protein sequence analysis from which the PCI domain was defined (3). We then cross-referenced this with protein alignment analyses of nearly all known Int6 proteins available to us at the time to identify those residues that are also conserved in these Int6 proteins (Fig. 5A, arrows). Site-directed mutagenesis was performed to alter them one by one. We then replaced the wild type *yin6* with the mutated ones and analyzed the phenotypes of the resulting cells. We have thus concluded that replacing the Leu at position 332 with aspartate (L332D) is particularly detrimental to the function of Yin6, as the cell carrying Yin6L332D displayed the same phenotype as *yin6*Δ cells (cold-dependent growth defect, abnormally fat and bent cell morphology, and hypersensitivity to canavanine; Fig. 6A and data not shown). In proteasome pull-down experiments, Yin6L332D did not efficiently bind the proteasome (Fig. 6A). An analogous mutation in human Int6 (Int6L312D) also inactivated Int6, since it could not rescue *yin6*Δ cells (Fig. 6B). These results are consistent with the idea that the Yin6L332D mutant loses its ability to bind and regulate the proteasome.

Since the first publication of the PCI sequence alignment, more PCI protein sequences have become available, and we have thus performed another alignment to identify Leu residues in other PCI proteins that might be structurally (and thus also functionally) analogous to L332 in Yin6 (Fig. 5B). Beside Yin6, we have characterized two more PCI proteins, Rpn5 and Rpn7, and the alignment data suggest that L316 in Rpn5 and L289 in Rpn7 are good candidates.

As shown in Fig. 6C, like *rpn5*Δ cells, the *rpn5L316D* mutant cells are hypersensitive to canavanine, and similarly Rpn7L289D was not as efficient as wild type Rpn7 in rescuing canavanine hypersensitivity of *rpn7*Δ cells (Fig. 6D). We have shown in this and previous study (14) that both Rpn5 and Rpn7 binds Rpn9. However, neither Rpn5L316D (Fig 6E) nor Rpn7L289D bound Rpn9 (Fig. 4D). To further ascertain whether these PCI mutations weakens the ability of these proteasome subunits to properly localize and assemble with the rest of the proteasome subunits in live cells, we analyzed the localization patterns of GFP-Rpn7L289D and GFP-Rpn7 in both wild type and *rpn7*Δ cells. Our data showed that while Rpn7 localized efficiently to the

nuclear envelope in both wild type and *rpn7*Δ cells (Fig. 6F), Rpn7L289D-GFP mislocalized throughout the cell in wild type cells and slightly mislocalized in the nucleoplasm of *rpn7*Δ cells. Rpn5L316D was similarly tested and yielded the same results (data not shown). These localization data suggest that the tested PCI mutant proteasome subunits are not nearly as efficient as their normal counterparts in localizing and assembling into the nuclear membrane and the proteasome; thus, the presence of the wild type versions easily competed out the assembly and localization of the mutant versions. Collectively, we conclude from these results that the identified Leu residue in the PCI domain plays a critical role in mediating the binding between PCI proteins in the proteasome, thus affecting how the proteasome is assembled and localized in the cell.

DISCUSSION

To better define the role of the PCI domain in proteasome functioning, we have isolated a new PCI-containing proteasome subunit, Rpn7, from *S. pombe*. Our data firmly support the idea that Rpn7 is a proteasome subunit because it associates with the proteasome, and because its inactivation appears to block the removal of polyubiquitinated proteins, as well as abnormal proteins that contain canavanine instead of arginine. Guided by protein sequence alignments, we performed structure-function analyses to identify in the PCI domain a Leu residue that is critical for the functions of at least three different PCI proteins. That is, Yin6L332D, Rpn5L316D, and Rpn7L289D cannot fully replace their wild type counterparts, and this observation correlates with the finding that they do not bind efficiently to the proteasome. These data support the hypothesis that the identified Leu residue is critical for many PCI domains to function properly.

Besides aspartic acid, we have mutated this Leu residue to an alanine in Yin6. The resulting mutant protein, albeit weaker than wild type Yin6, was more functional than those that carried the L to D substitution (data not shown). These data are consistent with the possibility that this Leu is in contact with other residues, residing either elsewhere in the PCI domain or in its binding partners, via hydrophobic interactions, which can be disrupted by the presence of an aspartate residue.

The Leu identified from this study corresponds to L121 in human e-IF3k, whose crystal structure has been reported. L121 resides at the end of the last pair of anti-parallel α-helices in the TPR-like sub-domain (α3 helix, red; Fig. 1A). Within a 5 Å radius of this Leu, five hydrophobic amino acid residues (L105, F117, W118, L128, and F134; Fig. 1B, purple) are so positioned that their side chains may interact with this Leu. While it is evident that most of these hydrophobic amino acids reside within the TPR-like sub-domain, F134 is in the WH sub-domain. It is thus possible that the identified Leu can modulate the proper folding and/or spatial arrangement either within the TPR-like sub-domain or between the TPR and the WH sub-domains by interacting with these hydrophobic side chains. The importance of such hydrophobic interaction is further supported by the observation that three of the five described potential hydrophobic partners (e.g., L105, F117, and F134) are highly conserved among many PCI proteins (Fig. 5B).

Isono and colleagues have identified a number of ts Rpn7 mutants in bud-

ding yeast (23). Each of these Rpn7 ts mutants contains more than one amino acid substitution, at least one of which in each mutant protein is in the PCI domain. Interestingly, none of these mutations can singularly inactivate budding yeast Rpn7; in contrast, mutating just the Leu identified in this study substantially weakens the function of *S. pombe* Rpn7. One interpretation of this is that by potentially modulating the conformation and folding of both the TPR-like and the WH subdomains, a substitution of this Leu to Asp may more globally and profoundly influence the structure of the PCI domain, thus leading to a greater loss of activity. We cannot exclude the possibility that this Leu may be part of a binding pocket, with which critical PCI binding partners interact.

Since each of the two sub-domains in the PCI domain contains ample surface for protein-protein interactions, it is reasonable to assume that the main role of the PCI domain is to assemble a protein complex. We have previously observed that the *S. pombe* lid PCI protein Rpn5 is grossly mislocalized only in the lid mutants, while in the base mutants, Rpn5 can at least still concentrate in the nucleus (14). A recent study of budding yeast proteasome has similarly shown that mutations affecting the lid, but not the base, lead to a grossly mislocalized lid (24). These results are consistent with the possibility that at least some components in the lid preferentially bind one another and that they do so in a highly cooperative manner. In this and other studies of ours (14), we found that both Rpn5 and Rpn7 preferentially bind Rpn9, and no other pair-wise binding can be detected between them. These results support the possibility that a complex consisting of Rpn5-Rpn9-Rpn7 can be found in *S. pombe*. A lid sub-complex containing Rpn5 and Rpn9 has indeed been found in budding yeast, although its Rpn7 does not seem to come in direct contact with Rpn9 (25).

ACKNOWLEDGEMENTS

We thank Chin-tung (Tommy) Chen for the expert help in the initial genetic screen and Gary Chamness for critically reading the manuscript. We also thank Nick Rhind, Chris Norbury, Roger Tsien, and Colin Gordon for kindly providing materials that are critical for this study. We truly appreciate Drs Wah Chiu and Matt Baker from the National Center for Macomolecular Imaging at Baylor College of Medicine for the computational assistance. Molecular graphics images were produced using the UCSF Chimera package from the Resource for Biocomputing, Visualization, and Informatics at the University of California, San Francisco (supported by NIH P41 RR-01081). ECC is supported by grants from the NIH (CA90464 and CA107187), DOD (BC021935), and Susan Komen Foundation (PDF0402733). ZS is supported by a DOD pre-doctoral fellowship (BC030443).

REFERENCES

1. Voges, D., Zwickl, P., and Baumeister, W. (1999) *Annu. Rev. Biochem* **68**, 1015-1068
2. Aravind, L., and Ponting, C. P. (1998) *Protein Sci* **7**(5), 1250-1254
3. Hofmann, K., and Bucher, P. (1998) *Trends Biochem. Sci.* **23**, 204-205
4. Chang, E. C., and Schwechheimer, C. (2004) *EMBO Rep.* **5**(11), 1041-1045
5. Wei, Z., Zhang, P., Zhou, Z., Cheng, Z., Wan, M., and Gong, W. (2004) *J Biol Chem* **279**(33), 34983-34990
6. Scheel, H., and Hofmann, K. (2005) *BMC Bioinformatics* **6**, 71
7. Yen, H.-c. S., and Chang, E. C. (2000) *Proc. Natl. Acad. Sci. USA* **97**(26), 14370-14375
8. Marchetti, A., Buttitta, F., Miyazaki, S., Gallahan, D., Smith, G., and Callahan, R. (1995) *J. Virol.* **69**, 1932-1938
9. Yen, H. C., and Chang, E. C. (2003) *Cell Cycle* **2**(2), 81-83
10. Sap, J., and Chang, E. C. (2005) *AfCS-Nature Signaling Gateway _ Molecule Pages* **doi:10.1038/mp.a003493.01**
11. Asano, K., Merrick, W. C., and Hershey, J. W. (1997) *J. Biol. Chem.* **272**, 23477-23480
12. Bandyopadhyay, A., Lakshmanan, V., Matsumoto, T., Chang, E. C., and Maitra, U. (2002) *J. Biol. Chem.* **277**(3), 2360-2367.
13. Yen, H. C., Gordon, C., and Chang, E. C. (2003) *Cell* **112**(2), 207-217
14. Yen, H. C., Espiritu, C., and Chang, E. C. (2003) *J. Biol. Chem.* **278**(33), 30669-30676
15. Norbury, C., and Moreno, S. (1997) *Methods Enzymol* **283**, 44-59
16. Wood, V., Gwilliam, R., Rajandream, M. A., Lyne, M., Lyne, R., Stewart, A., Sgouros, J., Peat, N., Hayles, J., Baker, S., Basham, D., Bowman, S., Brooks, K., Brown, D., Brown, S., Chillingworth, T., Churcher, C., Collins, M., Connor, R., Cronin, A., Davis, P., Feltwell, T., Fraser, A., Gentles, S., Goble, A., Hamlin, N., Harris, D., Hidalgo, J., Hodgson, G., Holroyd, S., Hornsby, T., Howarth, S., Huckle, E. J., Hunt, S., Jagels, K., James, K., Jones, L., Jones, M., Leather, S., McDonald, S., McLean, J., Mooney, P., Moule, S., Mungall, K., Murphy, L., Niblett, D., Odell, C., Oliver, K., O'Neil, S., Pearson, D., Quail, M. A., Rabbinowitsch, E., Rutherford, K., Rutter, S., Saunders, D., Seeger, K., Sharp, S., Skelton, J., Simmonds, M., Squares, R., Squares, S., Stevens, K., Taylor, K., Taylor, R. G., Tivey, A., Walsh, S., Warren, T., Whitehead, S., Woodward, J., Volckaert, G., Aert, R., Robben, J., Grymonprez, B., Weltjens, I., Vanstreels, E., Rieger, M., Schafer, M., Muller-Auer, S., Gabel, C., Fuchs, M., Fritzc, C., Holzer, E., Moestl, D., Hilbert, H., Borzym, K., Langer, I., Beck, A., Lehrach, H., Reinhardt, R., Pohl, T. M., Eger, P., Zimmermann, W., Wedler, H., Wambutt, R., Purnelle, B., Goffeau, A., Cadieu, E., Dreano, S., Gloux, S., Lelaure, V., Mottier, S., Galibert, F., Aves, S. J., Xiang, Z., Hunt, C., Moore, K., Hurst, S. M., Lucas, M., Rochet, M., Gaillardin, C., Tallada, V. A., Garzon, A., Thode, G., Daga, R. R., Cruzado, L., Jimenez, J., Sanchez, M., del Rey, F., Benito, J., Dominguez, A., Revuelta, J. L., Moreno, S., Armstrong, J., Forsburg, S. L., Cerrutti, L., Lowe, T., McCombie, W. R., Paulsen, I., Potashkin, J., Shpakovski, G. V., Ussery, D., Barrell, B. G., and Nurse, P. (2002) *Nature* **415**(6874), 871-880.

17. Chang, E. C., Barr, M., Wang, Y., Jung, V., Xu, H., and Wigler, H. M. (1994) *Cell* **79**, 131-141
18. Sivakumar, S., Porter-Goff, M., Patel, P. K., Benoit, K., and Rhind, N. (2004) *Methods* **33**(3), 213-219
19. Shu, X., Shaner, N. C., Yarbrough, C. A., Tsien, R. Y., and Remington, S. J. (2006) *Biochemistry* **45**(32), 9639-9647
20. Bähler, J., Wu, J. Q., Longtine, M. S., Shah, N. G., McKenzie, A., 3rd, Steever, A. B., Wach, A., Philippsen, P., and Pringle, J. R. (1998) *Yeast* **14**(10), 943-951
21. Janke, C., Magiera, M. M., Rathfelder, N., Taxis, C., Reber, S., Maekawa, H., Moreno-Borchart, A., Doenges, G., Schwob, E., Schiebel, E., and Knop, M. (2004) *Yeast* **21**(11), 947-962
22. Alfa, C., Fantes, P., Hyams, J., McLeod, M., and Warbrick, E. (1993) *Experiments with Fission Yeast*, Cold Spring Harbor Press, Cold Spring Harbor
23. Isono, E., Saeki, Y., Yokosawa, H., and Toh-e, A. (2004) *J Biol Chem* **279**(26), 27168-27176
24. Isono, E., Nishihara, K., Saeki, Y., Yashiroda, H., Kamata, N., Ge, L., Ueda, T., Kikuchi, Y., Tanaka, K., Nakano, A., and Toh, E. A. (2007) *Mol Biol Cell* **18**(2), 569-580
25. Sharon, M., Taverner, T., Ambroggio, X. I., Deshaies, R. J., and Robinson, C. V. (2006) *PLoS Biol.* **4**(8), 1314-1323.
26. Pettersen, E. F., Goddard, T. D., Huang, C. C., Couch, G. S., Greenblatt, D. M., Meng, E. C., and Ferrin, T. E. (2004) *J. Comput. Chem.* **25**(13), 1605-1612
27. DeLano, W. L. (2002). http://www.pymol.org.
28. Thompson, J. D., Higgins, D. G., and Gibson, T. J. (1994) *Nucleic Acids Res.* **22**, 4673-4680.

FOOTNOTES

[1]**The abbreviations used are:** PCI, Proteasome-COP9-Initiation factor; WH, winged-helix; e-IF3, eukaryotic initiation factor-3; TPR, Tetratrico Peptide Repeat; HAM, HEAT analogous motif; HEAT, Huntington elongation factor 3, a subunit of protein phosphatase 2A; PCR, polymerase chain reaction.

FIGURE LEGENDS

FIG. 1: 3D structure of the PCI domain in human e-IF3k. *A,* The N-terminal TPR/HAM sub-domain is colored green, while the C-terminal WH sub-domain is colored yellow. The described leucine residue corresponds to L121 (red) in e-IF3k, and is located at the end of the α3 helix in the N-terminal TPR/HAM sub-domain. Three helices from the TPR-like sub-domain and one helix from the WH sub-domain (arrow heads) contain hydrophobic amino acid residues that may interact with L121 (see *B*). *B,* Within a 5 Å

radius from this leucine, at least 5 hydrophobic amino acids colored in purple (L105, F117, W118, L128, and F134) can be readily identified that may interact this leucine. We note that while most of these neighboring hydrophobic residues reside in the TPR/HAM domain, F134 is in the WH domain. These images were created by the Chimera (26) and PyMOL (27) software.

FIG. 2: Rpn7 is a high copy suppressor that rescues *yin6*Δ phenotypes. *A, yin6*Δ cells (strain YIN6K) were transformed with either a vector control (pREP1) or the same vector carrying the *yin6* or *rpn7* (pREP1YIN6 or pREP1RPN7). Serially diluted cells were spotted on MM plates and incubated at indicated temperatures. *B,* Upper Panel: the same transformed *yin6*Δ cells as in *A* were pre-grown in MM at 32°C, and equal numbers were spread on MM plates with the indicated amount of canavanine and incubated at 32°C for 10 days. The number of colonies that emerged without canavanine was taken as 100% survival. Lower Panel: the same transformed *yin6*Δ cells as in *A* were serially diluted and spotted on MM plates with the indicated concentrations of canavanine, and incubated at 32°C.

FIG. 3. Rpn7 is an essential protein required for proteasome functioning. *A, rpn7*Δ/+ diploid cells were sporulated, and the resulting tetrads were dissected and their spores incubated at 30°C. A total of 16 tetrads were dissected, and 5 are shown in the figure. Only 2 out of the four spores in a given tetrad formed colonies, and they were all Ura^-. *rpn7*Δ spores could only divide a few times after germination and then stopped. *B, rpn7^{ts}* cells were grown in YEAU at 30°C, an intermediate temperature at which the cell showed mitotic defects although they did manage to grow, and stained with DAPI. Cells with fragmented chromosomes (left) or unevenly distributed chromosomes (middle and right) were readily observed for *rpn7^{ts}* cells. Arrowheads mark the septa. *C, rpn7^{ts}* and WT cells were serially diluted and spotted on MM plates with indicated concentration of canavanine, and grown at 25°C. *D,* Cell lysates were prepared from *rpn7^{ts}* and WT cells pre-grown at 30°C, then shifted to either 30 or 37°C for 12 hours. The levels of poly-ubiquitinated proteins were analyzed by Western blotting using an anti-Ub antibody. Coomassie Blue staining was used as the loading control.

FIG. 4. Rpn7 associates with the proteasome and preferentially binds Rpn9. *A,* mcRFP-Rpn7 was expressed from pMCRPN7 in strains (RPN11GFP and A4GFP) in which Rpn11 or α4 (not shown) was tagged with GFP. The green and red images were deconvolved and merged by the Slidebook software. The co-localization was further confirmed by examining each optical section manually. *B,* Endogenous Rpn7 in various strains was tagged by GFP, and the cells were grown in MM at 30°C and photographed. The strains used in this experiment were: RPN7GFP, Y6AR7GFP, and R5AR7GFP. *C,* Cell lysate from strain R10PAR7GFP, whose Rpn10/Pus1 proteasome subunit was tagged with protein A, were pulled-down with the IgG bead or the control protein A bead. The pulled-down proteins were analyzed by Western blots using antibodies specific for proteins as indicated on the right. *D,* Proteins fused with the LexA DNA binding domain (LBD) and the Gal4 activation domain (GAD) for the yeast two-hybrid assay are as indicated, and the activation of both *HIS3* and *lacZ* reporters is shown. The plasmids used to express fusion Rpn7 and Rpn9 proteins are pGADRPN9 (13), pLBDRPN7 and

pLBDRPN7LD. pVJL11 and pGADgh were used as vector controls, while pGADYIN6 and pLBDMOE1 were used as positive controls (7).

FIG. 5. Sequence alignment of the PCI region among *int6* genes, and among genes encoding PCI proteins. *A,* Sequence alignment was performed using the Clustal W program (28) to seek evolutionarily conserved amino acid residues in the PCI domains of many Int6 proteins. Arrows indicate residues that have been chosen as targets for mutagenesis and the red arrow marks the described leucine residue that is critical for Yin6 function. *B,* Sequence alignment of a number of genes encoding PCI proteins across different species was performed as described (6). The red rectangle encloses the residues corresponding to the identified conserved Leucine. Purple asterisks mark those hydrophobic residues that may interact with L121 as revealed in Fig. 1B. *S. pombe* Rpn5 and Rpn7 are marked by red arrows. The boundaries of the α3 helix (Fig 1A), the end of the HAM sub-domain, and the beginning of the WH sub-domain are marked with vertical lines. Residues that are part of a helix is marked with a "H".

FIG. 6: Identification of an essential leucine residue in three PCI domains. *A,* Left: Various strains were pregrown in YEAU at 30°C to log phase. Equal numbers of cells were spread on MM plates without or with 12 μg/ml canavanine sulfate and incubated at 30°C for 14 days. For each strain, the number of colonies that emerged on plates without canavanine was taken as 100% survival. The specific strains used: SP870 (WT), YIN6K (*yin6*Δ) and YIN6LD (*yin6L332D*). Right: Cells whose Rpn10 is tagged with protein A were transformed with pHA-YIN6 or pHA-YIN6LD and lysates were prepared and pulled-down with either IgG or control protein A beads. The pulled-down proteins were analyzed by Western blots using antibodies specific for either HA or Rpn10. *B,* The same number of *yin6*Δ cells (strain YIN6K) transformed with a vector control (pSLF173) or the same vector carrying the indicated genes (pHAYIN6, pHAHINT6 and pHAHINT6LD) were spread on MM plates and incubated at 20°C for 6 days. The growth of wild-type cells was unaffected by wild-type or mutated *yin6* expression (data not shown). *C,* There are two copies of *rpn5* genes, *rpn5a* and *rpn5b*. Equal number of cells from strains with indicated genotype were spread on MM plates containing indicated concentration of canavanine sulfate. The plates were incubated at 30°C. The specific strains used for this study were (Experimental procedures and ref. 14): SP870 (WT), RPN5LD (*rpn5aL316D-HA rpn5b*Δ), RPN5bARPN5aHA (rpn5a-HA rpn5bΔ), and RPN5UA (rpn5aΔ rpn5bΔ). *D,* WT or *rpn7*Δ cells were transformed with the vector control (-, pREP41) or the same vector expressing the indicated genes (pREP41Rpn7 and pREP41RPN7LD). The transformed cells were then serially diluted and spotted on MM plates containing the indicated concentration of canavanine and incubated at 30°C for 5 days. The expression of the gene was turned off by adding thiamine (20 μM). *E,* Hybrid proteins fused with the LexA DNA binding domain (LBD) and the Gal4 activation domain (GAD) are as indicated, and the activation of both *HIS3* and *lacZ* is shown. The plasmids used for expressing these fusion genes are: pGADRPN9, pLBDRPN5, and pLBDRPN5LD. *F,* WT or *rpn7*Δ cells were transformed with linearized pREPGFPRPN7 or pREPGFPRPN7LD to allow integration of these plasmids to the chromosome. These cells were grown in YEAU at 30°C to log phase before being photographed. The images were captured under identical conditions to reveal the different intensities of GFP signals between samples.

Supplemental Figures

FIG S1: Abnormal protein levels and localization of the ts Rpn7-GFP protein. *A,* Cells expressing either properly tagged Rpn7-GFP or improperly tagged Rpn7-GFP, called Rpn7-GFP^{ts}, were cultured in YEAU at 30°C and then photographed under identical camera setting. *B,* Lysates were prepared from cells used in *A,* or control cells containing no GFP tagged protein, and analyzed by Western Blotting with indicated antibodies. Relative GFP levels as normalized against actin were indicated under the WB. At this semi-permissive temperature, Rpn7-GFP^{ts} was already mislocalized in the nucleoplasm and its protein levels were greatly reduced.

FIG S2: Validation of a rabbit antibody against *S. pombe* α4 proteasome subunit. Lysates were prepared from two strains, one of which whose endogenous α4 subunit was tagged by GFP and one of which whose Rpn11 was tagged with GFP. Western blots were performed using antibodies that are shown at the bottom of each blot. Our serum against the α4 subunit recognized the 28 kDa endogenous α4 subunit (marked by #1) and the 55 kDa GFP-tagged version (marked by #2). #3 marks the 63 kDa Rpn11-GFP. The asterisk marks presumably free GFP protein, cleaved off from α4-GFP.

Figure 1

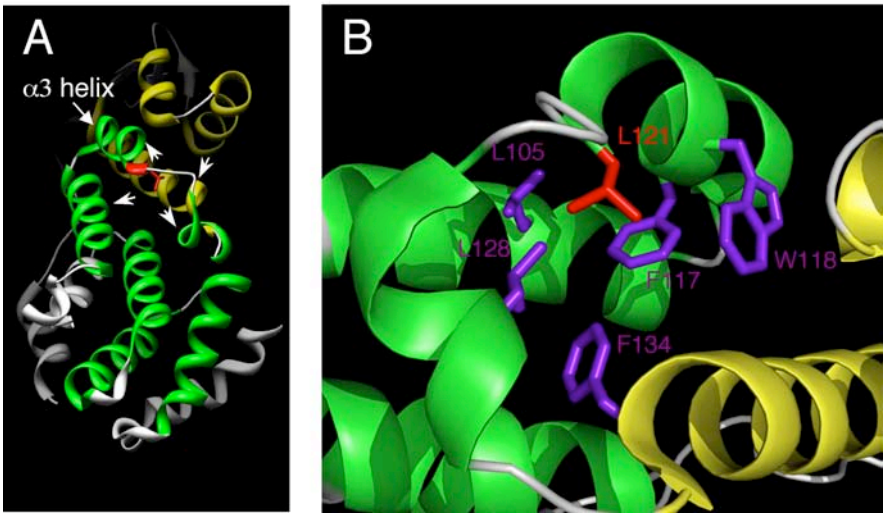

Figure 2

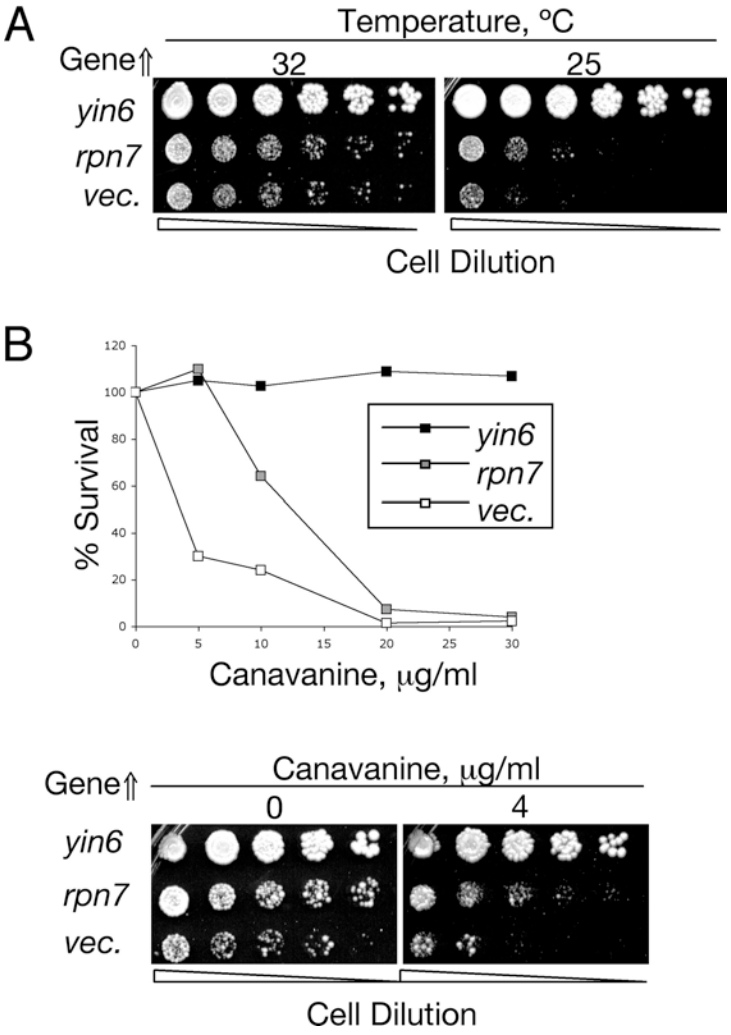
A
Temperature, °C
Gene⇑
32
25
yin6
rpn7
vec.
Cell Dilution
B
% Survival
120
100
80
60
40
20
0
0
5
10
15
20
25
30
yin6
rpn7
vec.
Canavanine, μg/ml
Gene⇑
Canavanine, μg/ml
0
4
yin6
rpn7
vec.
Cell Dilution

Figure 3

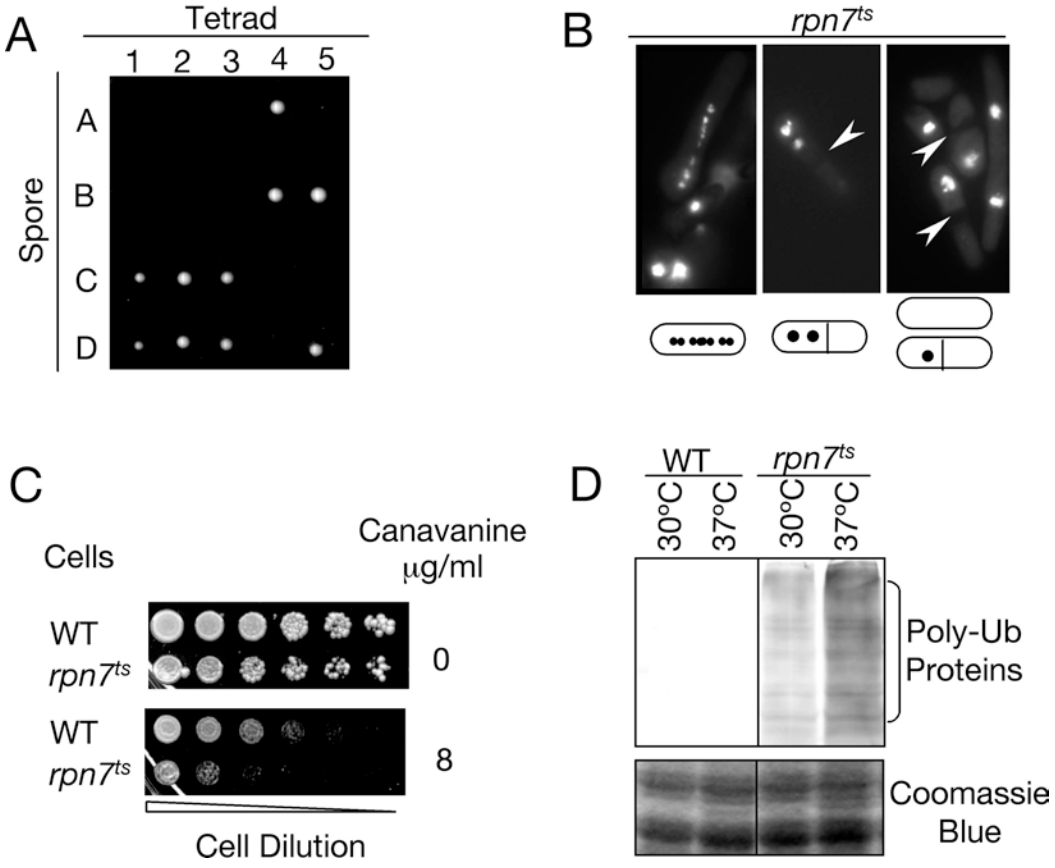
A
Tetrad
1 2 3 4 5
Spore
A
B
C
D
B
rpn7ts
C
Cells
Canavanine μg/ml
WT
rpn7ts
0
WT
rpn7ts
8
Cell Dilution
D
WT
rpn7ts
30°C
37°C
30°C
37°C
Poly-Ub Proteins
Coomassie Blue

Figure 4

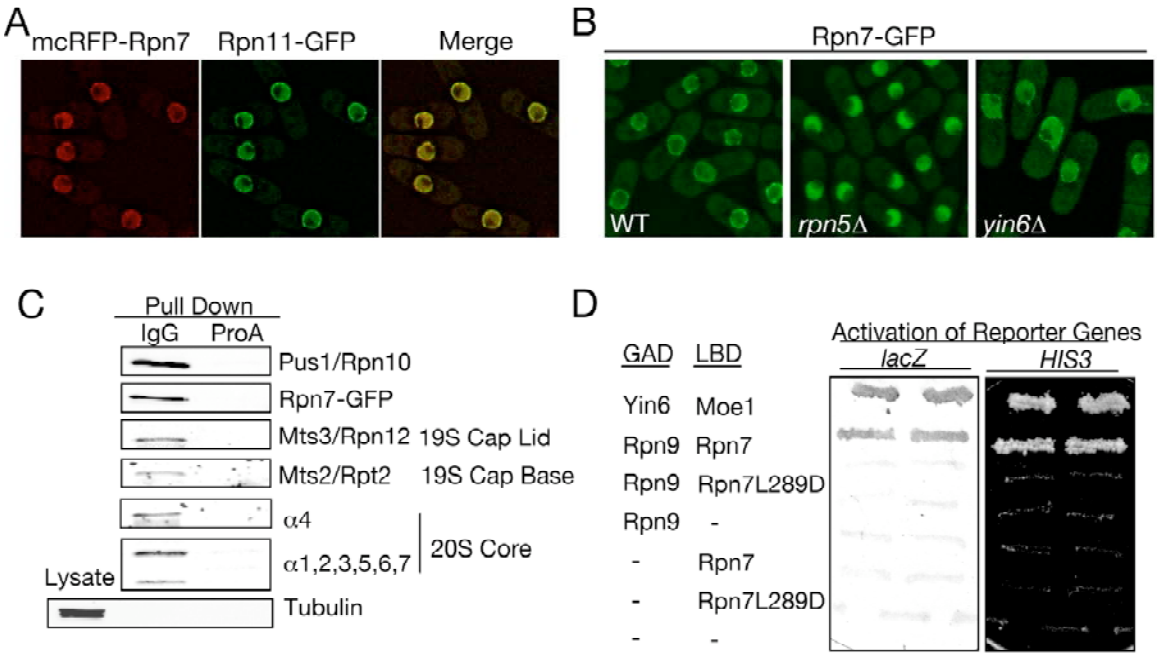
A
mcRFP-Rpn7
Rpn11-GFP
Merge
B
Rpn7-GFP
WT
rpn5Δ
yin6Δ
C
Pull Down
IgG
ProA
Pus1/Rpn10
Rpn7-GFP
Mts3/Rpn12
19S Cap Lid
Mts2/Rpt2
19S Cap Base
α4
α1,2,3,5,6,7
20S Core
Lysate
Tubulin
D
GAD
LBD
Activation of Reporter Genes
lacZ
HIS3
Yin6
Moe1
Rpn9
Rpn7
Rpn9
Rpn7L289D
Rpn9
-
-
Rpn7
-
Rpn7L289D
-
-

Figure 5

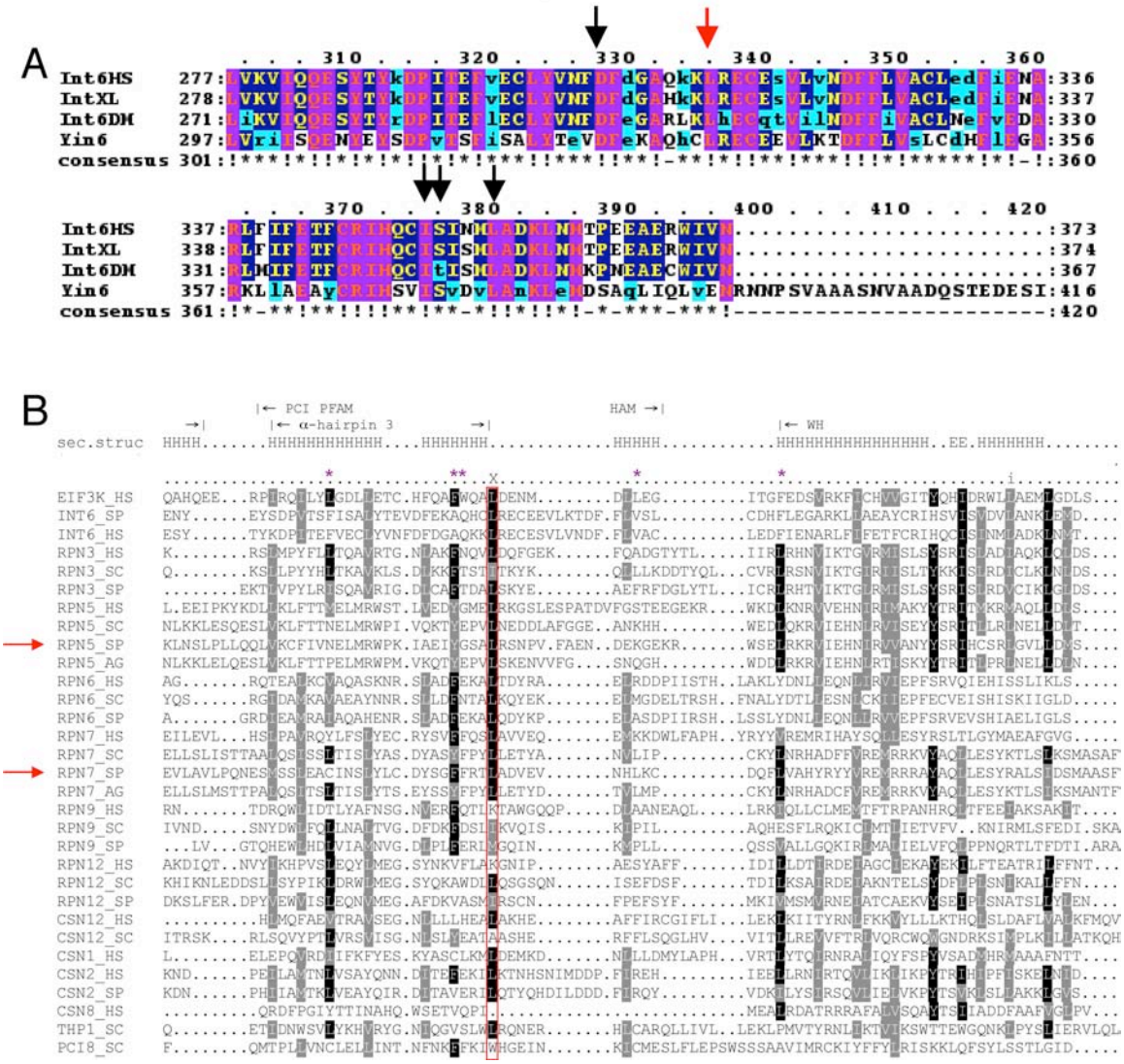
A
B
Int6HS
IntXL
Int6DM
Yin6
consensus
EIF3K_HS
INT6_SP
INT6_HS
RPN3_HS
RPN3_SC
RPN3_SP
RPN5_HS
RPN5_SC
RPN5_SP
RPN5_AG
RPN6_HS
RPN6_SC
RPN6_SP
RPN7_HS
RPN7_SC
RPN7_SP
RPN7_AG
RPN9_HS
RPN9_SC
RPN9_SP
RPN12_HS
RPN12_SC
RPN12_SP
CSN12_HS
CSN12_SC
CSN1_HS
CSN2_HS
CSN2_SP
CSN8_HS
THP1_SC
PCI8_SC

Figure 6

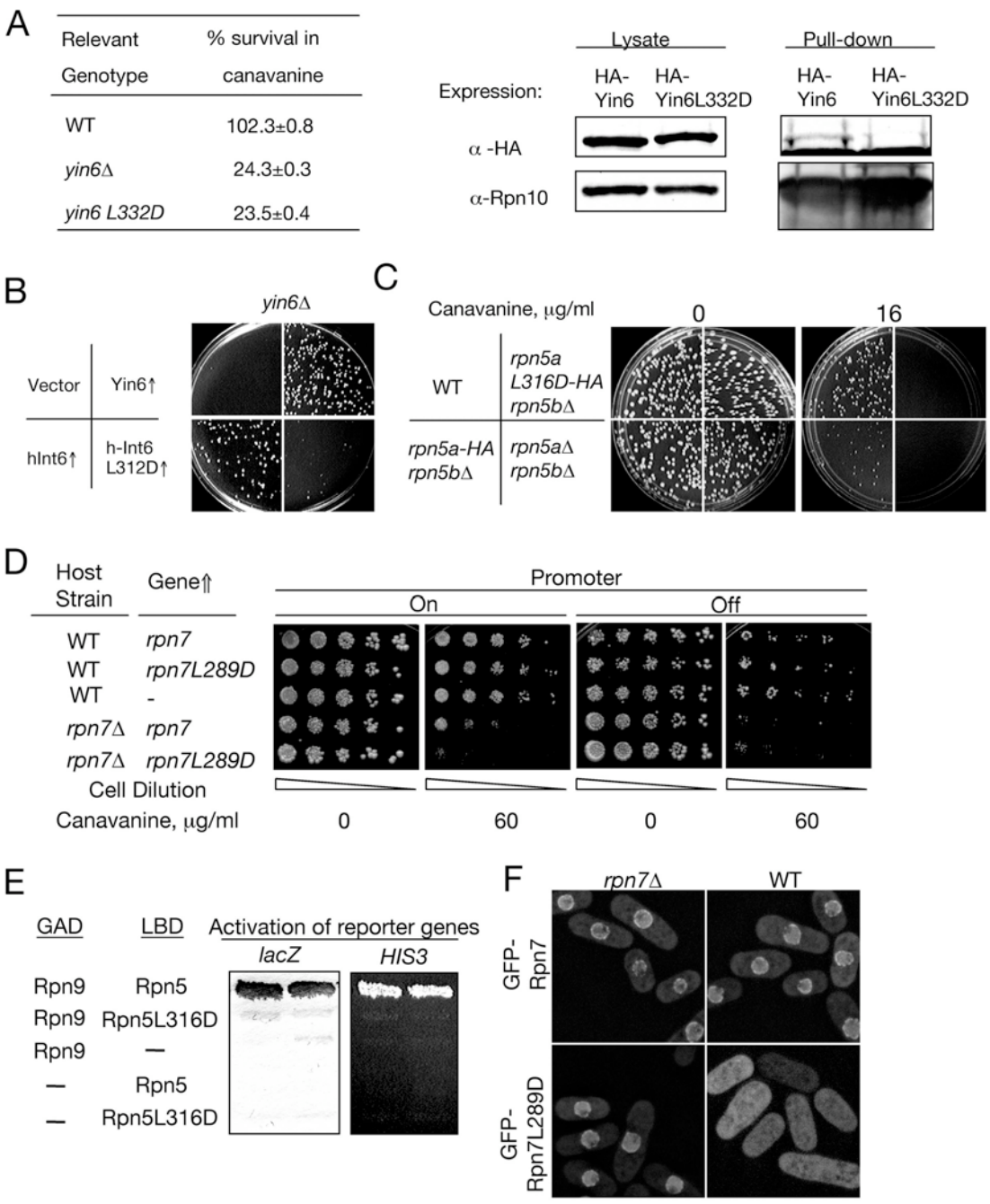
A
Relevant Genotype
% survival in canavanine
WT
102.3±0.8
yin6Δ
24.3±0.3
yin6 L332D
23.5±0.4
Lysate
Pull-down
Expression:
HA-Yin6
HA-Yin6L332D
α -HA
α-Rpn10
B
yin6Δ
Vector
Yin6↑
hInt6↑
h-Int6 L312D↑
C
Canavanine, μg/ml
0
16
WT
rpn5a L316D-HA rpn5bΔ
rpn5a-HA rpn5bΔ
rpn5aΔ rpn5bΔ
D
Host Strain
Gene⇑
Promoter
On
Off
WT rpn7
WT rpn7L289D
WT -
rpn7Δ rpn7
rpn7Δ rpn7L289D
Cell Dilution
Canavanine, μg/ml
0
60
0
60
E
GAD
LBD
Activation of reporter genes
lacZ
HIS3
Rpn9 Rpn5
Rpn9 Rpn5L316D
Rpn9 —
— Rpn5
— Rpn5L316D
F
rpn7Δ
WT
GFP-Rpn7
GFP-Rpn7L289D

Figure S1

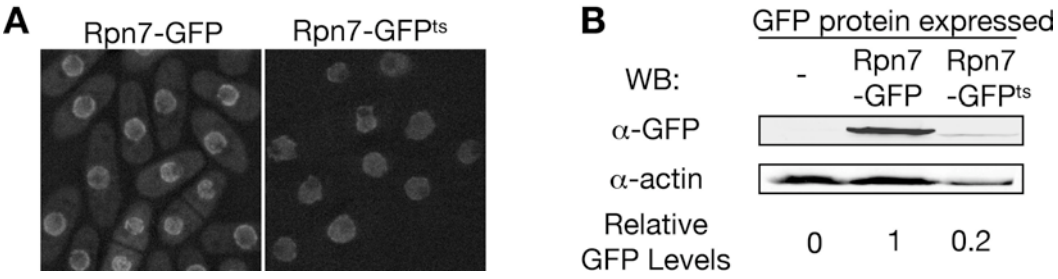

Figure S2